Author/s:
Zhou, R;Ji, M

Title:
Modelling Mortality Dependence: An Application of Dynamic Vine Copula

Date:
2021

Citation:
Zhou, R. & Ji, M. (2021). Modelling Mortality Dependence: An Application of Dynamic Vine Copula. Insurance: Mathematics and Economics, 99, pp.241-255. https://doi.org/10.1016/j.insmatheco.2021.03.022.

Modelling Mortality Dependence: An Application of Dynamic Vine Copula

Rui Zhou[1] and Min Ji[2]

[1]Department of Economics, University of Melbourne
[2]Department of Mathematics, Towson University

September 10, 2020

Abstract

Vine copula, constructed from bivariate copulas, provides great flexibility in modelling complex high-dimensional dependence. When applied to multi-population mortality modelling, vine copula yields significant improvement over traditional multivariate copulas. In this paper, we propose to capture time-varying features in mortality dependence with dynamic regular vine (R-vine) copula which is built from bivariate copulas with time-varying dependence parameters. We develop two dependence dynamics for R-vine copulas and illustrate the selection and estimation of dynamic R-vine copulas using mortality data from eight populations. The estimated R-vine copulas using the proposed dependence dynamics are shown to yield better goodness of fit than both static and regime-switching vine copulas. We further demonstrate the simulation of mortality paths using dynamic R-vine copulas and examine the impact of vine copula choice on the assessed effectiveness of longevity hedge.

Keywords: Vine copula; Time-varying dependence; Mortality dependence; Multi-population mortality modelling; Longevity hedge

1 Introduction

Multi-population mortality models are developed for and applied to business problems in which mortality dependence among populations plays an important role. For instance, an annuity provider plans to hedge the longevity risk in its annuity portfolio with standardized longevity instrument. The hedge involves two populations, of which one underlies the hedging instrument and the other is associated with the annuity liability. The mortality dependence between the two populations determines the effectiveness of the longevity hedge. Therefore, it is imperative to model the mortality dependence adequately prior to evaluating the hedge effectiveness.

Existing multi-population mortality models can be approximately categorized into two groups. The first group, including Cairns et al. [2011], Dowd et al. [2011], Li and Hardy [2011], Li et al. [2015], Li and Lee [2005], Yang and Wang [2013], Zhou et al. [2013], and Zhou et al. [2014], utilizes multivariate time series models such as vector autoregressive model to capture the auto-correlation and cross-correlation in the multi-population mortality data. The other group, including Wang et al. [2015], Chen et al. [2015], Chuliá et al. [2016], Chen et al. [2017], and Zhou [2019], applies multivariate copula approaches to capture non-linear and asymmetric mortality dependence. In this paper, we adopt the copula approach which allows us to separately estimate marginal models and dependence structure. Since single-population mortality models have been well studied [Cairns et al., 2009] and can be readily applied as the marginal models in the copula approach, we focus on the development of a suitable copula for the dependence structure.

Copula approach has been widely used in finance and insurance literature [Li, 2000, Rodriguez, 2007, Frees and Valdez, 2008, Czado et al., 2012a]. Classical multivariate copulas lack flexibility in modelling complex high-dimensional dependence. Multivariate elliptical copulas impose the same dependence structure between each pair of variables. Classical multivariate Archimedean copulas use only one parameter to capture the dependence among all variables. To achieve greater flexibility, Joe [1997], Embrechts et al. [2003], Whelan [2004], [Hofert, 2011], and Okhrin et al. [2013] study nested/hierarchical Archimedean copulas which are compositions of simple Archimedean copulas; Liebscher [2008] and Morillas [2005] introduce generalized multiplicative Archimedean copulas which are based on a second functional representation of Archimedean copulas via multiplicative generators; Aas et al. [2009] and Dißmann et al. [2013] propose vine copulas using pair copulas as the building blocks and vine as the construction method. Fischer et al. [2009] compare the performance of the aforementioned classes of multivariate copulas and observe that pair-copula construction proposed by Aas et al. [2009] outperforms the other copula classes in modelling the dependence of high-dimensional financial return data.

In this paper, we adopt regular vine copula to model mortality dependence. Regular vine (R-vine), defined in Bedford and Cooke [2001, 2002], is a graphical model to decompose joint density into products of marginal densities and bivariate copula densities. Since a large number of decompositions are possible using R-vine and an arbitrary bivariate copula is allowed for each edge in the vine, R-vine copula is very flexible in constructing high-dimensional dependence. Vine copula has been successfully employed to model dependence in various datasets, including financial asset returns [Brechmann and Czado, 2013, Dißmann et al., 2013], exchange rates [Czado et al., 2012b], precious metal prices [Reboredo and Ugolini, 2015], and daily mean temperatures [Erhardt et al., 2015]. Applications of vine copula in mortality modelling only emerged very recently. Chuliá et al. [2016] use a vine copula to model the dependence between idiosyncratic factors identified by a factor copula from multiple mortality improvement rates. Zhou [2019] proposed a regime-switching vine copula to capture the changes of mortality dependence over time.

Our goal, similar with that of Zhou [2019], is to examine how mortality dependence evolves over time. We develop a dynamic vine copula that allows mortality dependence to change gradually over time. The time-varying dependence parameters are determined by an autoregressive term and a forcing variable. Similar dynamics were shown to improve the performance of factor copula and classical multivariate copula [Chen et al., 2017, Wang et al., 2015] when applied to mortality dependence.

The proposed dynamic vine copula differs from the regime-switching vine copula introduced by Zhou [2019] in the way that dependence changes. The former assumes that both vine structure and families of bivariate copulas associated with the vine remain unchanged over time while allowing bivariate copula parameters to vary in each period. The evolution of dependence parameters is determined by a function of an autoregressive term and a forcing variable. The latter assumes that vine structure remains unchanged while families and parameters of bivariate copulas used to construct the vine shift with regime. The switching of regime is governed by an unobservable Markov process. The families of bivariate copulas associated with the vine in each regime are identified through a rolling window analysis. However, this analysis does not always provide clear indication of how regime changes and thus may require subjective judgement.

Dynamic vine copula was first introduced by So and Yeung [2014] and applied to stock return data. The dependence dynamic proposed by So and Yeung [2014], which is also a function of an autoregressive term and a forcing variable, encounters two problems. First, this dynamic does not ensure that correlation coefficients are always in the interval of $[-1, 1]$. Secondly, no justification is given for forming the forcing variable with past two periods of data. We address the first problem by introducing suitable transformation functions such that the correlation coefficients always remain in the desired interval. We use Bayesian Information Criteria (BIC), a quantitative measure, to select the period of past data used in the forcing variable, thereby resolving the second problem. In addition to improving the dependence dynamic proposed by So and Yeung [2014], we also introduce an alternative forcing variable which is shown to yield better goodness of fit.

The estimation procedure set out by So and Yeung [2014] requires that vine structure and families of bivariate copulas associated with the vine are given and all bivariate copulas are dynamic. We present a generalized sequential selection and estimation procedure that requires no prior information of the vine. Our procedure can automatically select vine structure, choose between dynamic and static bivariate copulas, and estimate copula parameters.

We implement the copula approach to model multi-population mortality in the following steps:

1. Fit a base mortality model to the mortality data of each population and obtain estimated age, period and cohort components for each population.
2. Model the dynamics of estimated period components using ARIMA-GARCH-copula model
   (a) Select and estimate an ARIMA-GARCH model for the period components of each population and obtain the standardized residuals
   (b) Select and estimate a dynamic R-vine copula to capture the dependence among the series of standardized residuals

We illustrate the stepwise procedure using mortality data from eight populations. We propose two different dependence dynamics for R-vine copula and evaluate the performance of proposed dynamic R-vine copulas in model fitting and forecasting. We also set up an illustrative longevity hedge and examine how the choice of dependence structure impacts the assessed hedge effectiveness.

The remaining of this paper is organized as follows: Section 2 describes mortality data, base mortality model, and marginal model for the estimated period components; Section 3 introduces static R-vine copula and its estimation; Section 4 develops two dependence dynamics for R-vine copula and proposes a generalized selection and estimation procedure for dynamic vine copula; Section 5 evaluates the forecasts of future dependence generated by the proposed dynamic R-vine copulas; Section 6 examines the impact of copula choice on the effectiveness of longevity hedge; Section 7 compares dynamic vine copula with regime-switching vine copula; and Section 8 concludes.

2 Data and Mortality Model

2.1 Data

To illustrate the application of dynamic vine copula in modelling high-dimensional mortality dependence, we use the male mortality data from eight countries: (1) Italy, (2) France, (3) England and Wales, (4) Switzerland, (5) Sweden, (6) Finland, (7) Netherlands, and (8) Norway. The mortality data, obtained from the Human Mortality Database [2017], comprise numbers of deaths and numbers of exposures-at-risk for the sample age range of 50-89 and the sample period of 1900-2012. The sample age range and sample period are intentionally chosen to match those used in Zhou [2019] such that a comparison between regime-switching and dynamic vine copula can be performed.

2.2 Base mortality model

We use the age-period-cohort (APC) model [Osmond, 1985] as the base mortality model for its simplicity and robustness. Other mortality models such as Lee-Carter model, Cairns-Blake-Dowd model, and their variants [Cairns et al., 2009] can be easily adapted to our framework.

The APC model which decomposes mortality rate into age, period, and cohort components can be expressed as follows:

$$\ln m_{x,t}^{(i)} = \alpha_x^{(i)} + \kappa_t^{(i)} + \gamma_{t-x}^{(i)},$$

where $m_{x,t}^{(i)}$ is the central death rate of an individual aged x in year t from population (i), and $\alpha_x^{(i)}$, $\kappa_t^{(i)}$, and $\gamma_{t-x}^{(i)}$ represent the age, period, and cohort components respectively.

Denote $D_{x,t}^{(i)}$ and $E_{x,t}^{(i)}$ as the number of deaths and number of exposures-at-risk at age x in year t from population (i). Assuming that $D_{x,t}^{(i)}$ follows a Poisson distribution with mean equal to $m_{x,t}^{(i)}E_{x,t}^{(i)}$, we estimate the APC model by maximizing the following

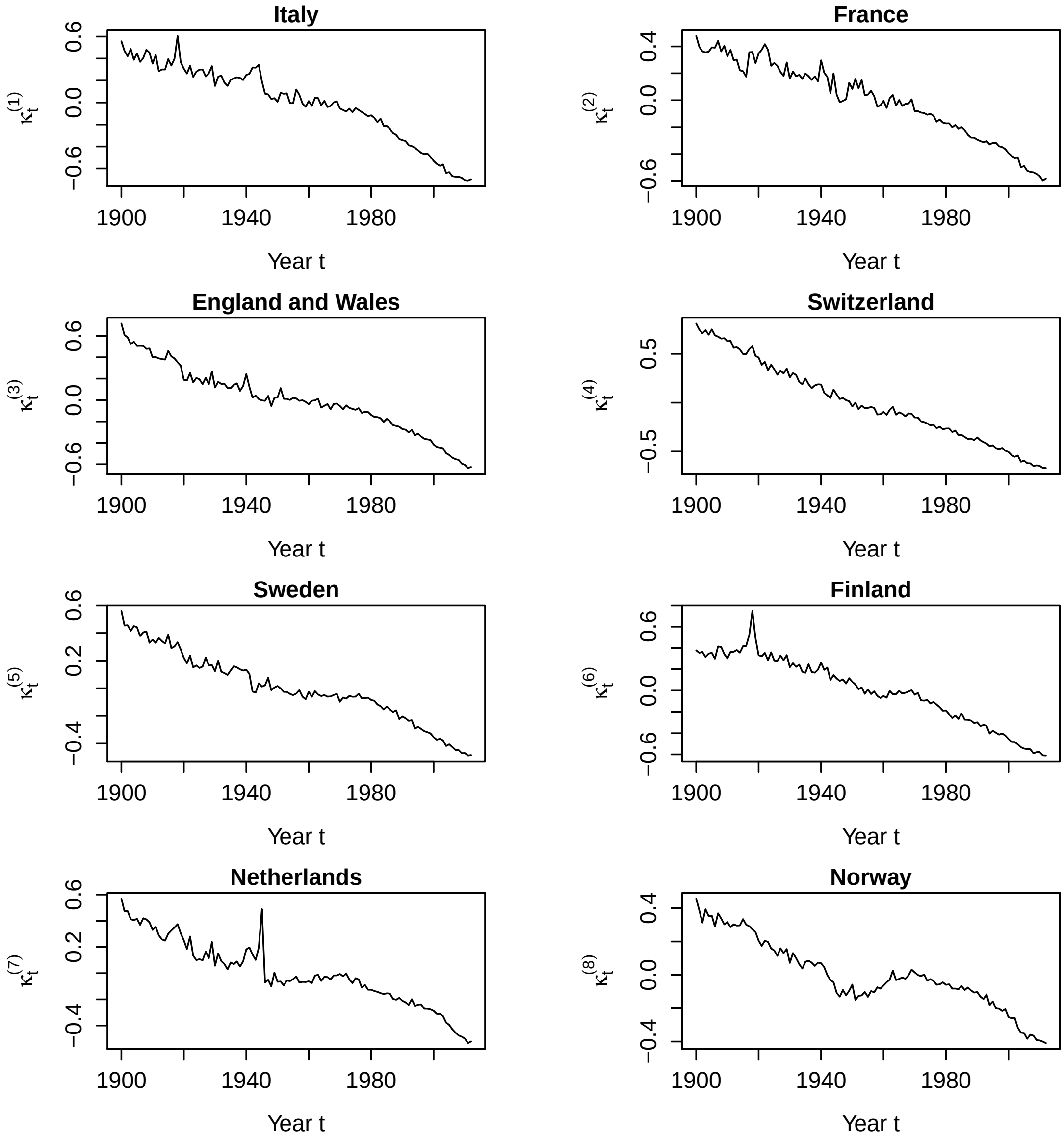

Figure 1: Estimated $\kappa_t^{(i)}$, $i = 1, 2, \ldots, 8$

loglikelihood function:

$$\sum_{x=50}^{89} \sum_{t=1900}^{2012} \left(D_{x,t}^{(i)} \ln(m_{x,t}^{(i)}) - m_{x,t}^{(i)} E_{x,t}^{(i)} \right) + \text{constant}.$$

To obtain unique parameter estimates, we impose three identification constraints: $\sum_{t=1900}^{2012} \kappa_t^{(i)} = 0$, $\sum_{t-x=1811}^{1962} \gamma_{t-x}^{(i)} = 0$, and $\sum_{t-x=1811}^{1962} (t-x)\gamma_{t-x}^{(i)} = 0$. The estimated period components $\{\kappa_t^{(i)}\}$, $i = 1, 2, \ldots, 8$, are displayed in Figure 1.

2.3 Marginal model for the estimated period components

The next step towards building the multi-population mortality model is to select a marginal model for each of the period component series. Since several researchers, including Chen et al. [2015], Chen et al. [2017], Lin et al. [2015] and Wang and Li. [2016], detect volatility heteroscedasticity in period components, we consider an ARIMA(p,d,q)-GARCH(P,Q) model for each estimated $\{\kappa_t^{(i)}\}$ series.

Figure 1 shows nearly linear downward trend in all period component series, thereby suggesting that the first difference of $\{\kappa_t^{(i)}\}$ may be stationary. Therefore, we perform the augmented Dickey-Fuller test on the first difference of each $\{\kappa_t^{(i)}\}$ series. Since the test always rejects the null hypothesis that a unit root is present, we select difference order of 1 for all estimated $\{\kappa_t^{(i)}\}$, $i = 1, 2, \ldots, 8$.

The ARIMA$(p,1,q)$-GARCH(P,Q) model for $\kappa_t^{(i)}$ is expressed as:

$$
\begin{aligned}
&\Delta\kappa_t^{(i)} + \sum_{l=1}^{p} \phi_l \Delta\kappa_{t-l}^{(i)} = \mu + \sum_{j=1}^{q} \theta_j \epsilon_{t-j+1}^{(i)},\\
&\epsilon_t^{(i)} = \sigma_t^{(i)} z_t^{(i)},\\
&\left(\sigma_t^{(i)}\right)^2 = \omega + \sum_{j=1}^{P} \beta_j \left(\sigma_{t-j}^{(i)}\right)^2 + \sum_{j=1}^{Q} \alpha_j \left(\epsilon_{t-j}^{(i)}\right)^2,
\end{aligned}
$$

where $\Delta\kappa_t^{(i)} = \kappa_t^{(i)} - \kappa_{t-1}^{(i)}$ and $z_t^{(i)} \sim i.i.d.(0,1)$. The parameters of GARCH volatility model are constrained by $\omega > 0$, $\alpha_j \geq 0$, $\beta_j \geq 0$, and $\sum_{j=1}^{Q} \alpha_j + \sum_{j=1}^{P} \beta_j < 1$ to ensure stationarity and positivity.

We select the AR and MA orders, (p,q), that yield the lowest Bayesian Information Criteria (BIC). The selected AR and MA orders are presented in Table 1. To examine the presence of volatility heteroscedasticity, we analyse the residuals $\{\epsilon_t^{(i)}\}$ obtained from fitting the selected ARIMA model to $\{\kappa_t^{(i)}\}$. We perform both ARCH test on the residuals and Ljung-Box test on the squared residuals. All the residual series except $\{\epsilon_t^{(5)}\}$ are found to exhibit volatility heteroscedasticity. For the residual series with significant ARCH effect, we further determine GARCH order and error distribution based on BIC. We consider three candidate GARCH orders: (1,0), (0,1), and (1,1); and nine candidate residual distributions: normal (Norm), skewed normal (SNorm), Student (Std), skewed Student, generalized error, skewed generalized error, generalized hyperbolic, normal inverse Gaussian, and Johnson's SU. The selected GARCH orders and residual distributions are presented in Table 1.

Given the orders of the ARIMA-GARCH model, the parameters of the model are estimated using maximum likelihood estimation (MLE) and summarized in Table 1. Note that "Shape" and "Skew" represent the shape and skew parameters in the residual distribution respectively. The standardized residuals $\{z_t^{(i)}\}$ obtained from the ARIMA-GARCH estimation will be used to construct a copula to depict the dependence of period components among the eight populations.

Series	$\kappa_t^{(1)}$	$\kappa_t^{(2)}$	$\kappa_t^{(3)}$	$\kappa_t^{(4)}$	$\kappa_t^{(5)}$	$\kappa_t^{(6)}$	$\kappa_t^{(7)}$	$\kappa_t^{(8)}$
(p,d,q)	(0,1,1)	(0,1,1)	(0,1,1)	(0,1,1)	(0,1,1)	(0,1,1)	(0,1,1)	(1,1,0)
μ	−0.015 (0.001)	−0.012 (0.002)	−0.014 (0.002)	−0.012 (0.001)	−0.009 (0.002)	−0.012 (0.001)	−0.006 (0.002)	−0.008 (0.002)
ϕ_1	-	-	-	-	-	-	-	−0.376 (0.100)
θ_1	−0.367 (0.086)	−0.427 (0.083)	−0.415 (0.073)	−0.576 (0.077)	−0.505 (0.084)	−0.475 (0.074)	−0.233 (0.075)	-
(P,Q)	(1,1)	(1,1)	(1,1)	(1,1)	(0,0)	(1,1)	(1,0)	(1,0)
ω	0.000 (0.000)	0.000 (0.000)	0.000 (0.000)	0.000 (0.000)	-	0.000 (0.000)	0.001 (0.000)	0.001 (0.000)
α_1	0.201 (0.093)	0.160 (0.079)	0.090 (0.049)	0.096 (0.084)	-	0.061 (0.103)	0.801 (0.199)	0.323 (0.165)
β_1	0.798 (0.071)	0.833 (0.055)	0.895 (0.044)	0.887 (0.109)	-	0.917 (0.095)	-	-
Shape	-	4.871 (1.817)	5.168 (2.429)	-	-	4.679 (1.741)	-	-
Skew	-	-	-	-	-	-	1.464 (0.209)	-
Distribution	Norm	Std	Std	Norm	-	Std	SNorm	Norm

Table 1: Estimated ARIMA-GARCH models for $\kappa_t^{(i)}$, $i = 1, 2 \ldots, 8$

3 Regular Vine Copula

3.1 Classical multivariate copulas

The Sklar theorem [Sklar, 1959] states that for n variables $Y_1, Y_2, \ldots, Y_n$ there exists an n-dimensional copula such that the joint cumulative distribution function (CDF), $F(y_1, y_2, \ldots, y_n)$, can be expressed as

$$F(y_1, y_2, \ldots, y_n) = C(F_1(y_1), F_2(y_2), \ldots, F_n(y_n)),$$

where $F_i(.)$ denotes the marginal CDF of Y_i and $C(.)$ is the copula CDF. The Sklar theorem allows us to construct a joint CDF by separately specifying the marginal distribution $F_i(Y_i)$ and the dependence structure $C(.)$. This approach is especially manageable when the marginal models of the variables under consideration have been extensively studied thereby leaving only the copula CDF to be specified. In the context of mortality modelling, single-population mortality models have been well researched and can be readily used as marginal models as demonstrated in Section 2. Therefore, our focus is to construct a suitable high-dimensional copula for mortality dependence.

Commonly used classical multivariate copulas, which are listed in Appendix A, can be used for modelling mortality dependence. However, these copulas have been criticized for their inflexibility in modelling complex high-dimensional dependence. In particular, multivariate elliptical copulas, including Gaussian and t copulas, impose the same dependence structure between each pair of variables; classical multivariate Archimedean copulas, including Clayton, Gumbel, Frank, and Joe copulas, use only one parameter to capture the dependence among all variables.

3.2 Regular vine copula

To build flexible high-dimensional copulas, Aas et al. [2009] proposed the pair-copula construction approach which utilizes vine and bivariate copulas. Vine, first proposed by Joe [1996] and further developed by Bedford and Cooke [2001, 2002], is a graphical tool that can be used to decompose join distribution into a product of marginal distributions and bivariate copulas linking the marginals.

A regular vine (R-vine) $\mathcal{V}$ on n variables is a sequence of $n-1$ connected trees $T_1, T_2, \ldots, T_{n-1}$ which satisfy the following properties [Bedford and Cooke, 2001, 2002]:

- T_1 is a tree with node set $N_1 = \{1, \ldots, n\}$ and edge set E_1.
- For $i = 2, \ldots, n-1$, T_i is a connected tree with node set $N_i = E_{i-1}$, of which the cardinality is $n-(i-1)$, and edge set E_i.
- The proximity condition: If two nodes in T_i, for $i = 2, \ldots, n-1$, are joined by an edge, their corresponding edges in T_{i-1} must share a common node.

Let us define bivariate copula density $c_{jk}(F_j(y_j), F_k(y_k))$ and conditional bivariate copula density $c_{jk;D}(F_{j|D}(y_j|\boldsymbol{y}_D), F_{k|D}(y_k|\boldsymbol{y}_D))$ as follows:

$$\begin{aligned}
c_{jk}(F_j(y_j), F_k(y_k)) &= \frac{\partial^2 C(F_j(y_j), F_k(y_k))}{\partial F_j(y_j)\partial F_k(y_k)}, \\
c_{jk;D}(F_{j|D}(y_j|\boldsymbol{y}_D), F_{k|D}(y_k|\boldsymbol{y}_D)) &= \frac{\partial^2 C(F_{j|D}(y_j|\boldsymbol{y}_D), F_{k|D}(y_k|\boldsymbol{y}_D))}{\partial F_{j|D}(y_j|\boldsymbol{y}_D)\partial F_{k|D}(y_k|\boldsymbol{y}_D)},
\end{aligned}$$

where D is the conditioning set and $\boldsymbol{y}_D = \{y_i | i \in D\}$. Bedford and Cooke [2001, 2002] demonstrate that the joint density function of $Y_1, \ldots, Y_n$ can be decomposed using a R-vine and expressed as follows:

$$f(y_1, \ldots, y_n) = \prod_{k=1}^{n} f_k(y_k) \times \prod_{i=1}^{n-1} \prod_{e \in E_i} c_{j,k;D}(F_{j|D}(y_j|\boldsymbol{y}_D), F_{k|D}(y_k|\boldsymbol{y}_D)), \tag{1}$$

where $e = \{j, k; D\}$ is an edge connecting node j and k, D is the conditioning set associated with the edge e, and $c_{j,k;D}(F_{j|D}(y_j|\boldsymbol{y}_D, F_{k|D}(y_k|\boldsymbol{y}_D)$ is the bivariate copula density associated with the edge e. The conditional distribution function, also commonly known as h-function, can be expressed as follows:

$$F_{j|D}(y_j|\boldsymbol{y}_D) = \frac{\partial C_{j,D_i;D_{-i}}\left(F_{j|D_{-i}}(y_j|\boldsymbol{y}_{D_{-i}}), F_{D_i|D_{-i}}(y_{D_i}|\boldsymbol{y}_{D_{-i}})\right)}{\partial F_{i|D_{-i}}(y_i|\boldsymbol{y}_{D_{-i}})}, \tag{2}$$

where D_i is the ith element in the set D and D_{-i} is the set D without the ith element.

There are $\frac{n!}{2} 2^{\frac{(n-2)(n-3)}{2}}$ possible n-dimensional R-vine structures, each of which corresponds to a unique decomposition of joint density function. For each edge in a R-vine, an arbitrary choice of bivariate copula is allowed. The large number of R-vine structures and arbitrary choice of bivariate copula families result in a vast collection of joint densities, thereby providing high flexibility in modelling complex dependences.

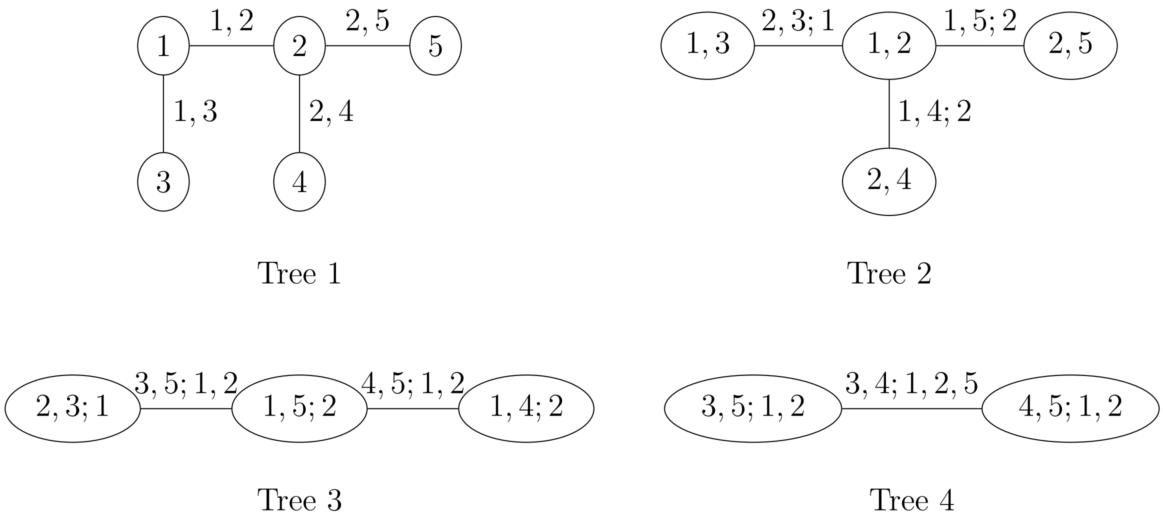

Figure 2: A illustrative five-dimensional R-vine structure

An illustrative five-dimensional R-vine is shown in Figure 2. In Tree 1, the node set is $N_1 = \{1, 2, 3, 4, 5\}$ and the edge set is $E_1 = \{\{1, 2\}, \{2, 5\}, \{1, 3\}, \{2, 4\}\}$. In Tree 2, the node set N_2 is equal to E_1. Nodes $\{1, 3\}$ and $\{1, 2\}$ in Tree 2 are joined by the edge $\{2, 3; 1\}$. Their corresponding edges in Tree 1 share a common node 1, thereby satisfying the proximity condition.

Using equation (1), the joint density function of five variables $Y_1, \ldots, Y_5$ satisfying the R-vine dependence shown in Figure 2 can be decomposed as follows:

$$
\begin{aligned}
f(y_1, \ldots, y_5) \quad = \quad & \prod_{k=1}^{5} f_k(y_k) \cdot c_{1,2}(F_1(y_1), F_2(y_2)) \cdot c_{1,3}(F_1(y_1), F_3(y_3)) \\
& \cdot c_{2,5}(F_2(y_2), F_5(y_5)) \cdot c_{2,4}(F_2(y_2), F_4(y_4)) \\
& \cdot c_{2,3;1}(F_{2|1}(y_2|y_1), F_{3|1}(y_3|y_1)) \cdot c_{1,5;2}(F_{1|2}(y_1|y_2), F_{5|2}(y_5|y_2)) \\
& \cdot c_{1,4;2}(F_{1|2}(y_1|y_2), F_{4|2}(y_4|y_2)) \cdot c_{3,5;1,2}(F_{3|1,2}(y_3|y_1, y_2), F_{5|1,2}(y_5|y_1, y_2)) \\
& \cdot c_{4,5;1,2}(F_{4|1,2}(y_4|y_1, y_2), F_{5|1,2}(y_5|y_1, y_2)) \\
& \cdot c_{3,4;1,2,5}(F_{3|1,2,5}(y_3|y_1, y_2, y_5), F_{4|1,2,5}(y_4|y_1, y_2, y_5))
\end{aligned} \tag{3}
$$

When the marginal distribution of Y_i is uniform on $[0, 1]$, we have $f_k(y_k) = 1$ and equation (3) reduces to the product of bivariate copula densities.

3.3 R-vine copula selection and estimation

Due to the large number of possible R-vine structures, it is very time consuming to consider all the structures in the selection process. Dißmann et al. [2013] proposed a sequential selection and estimation method which aims to capture as much dependence as possible at the lower layers of a R-vine, thereby leaving little or no dependence to be modelled at the higher layers. More specifically, the following steps are performed sequentially for $i = 1, 2, \ldots, n - 1$ to select and estimate an n-dimensional R-vine copula:

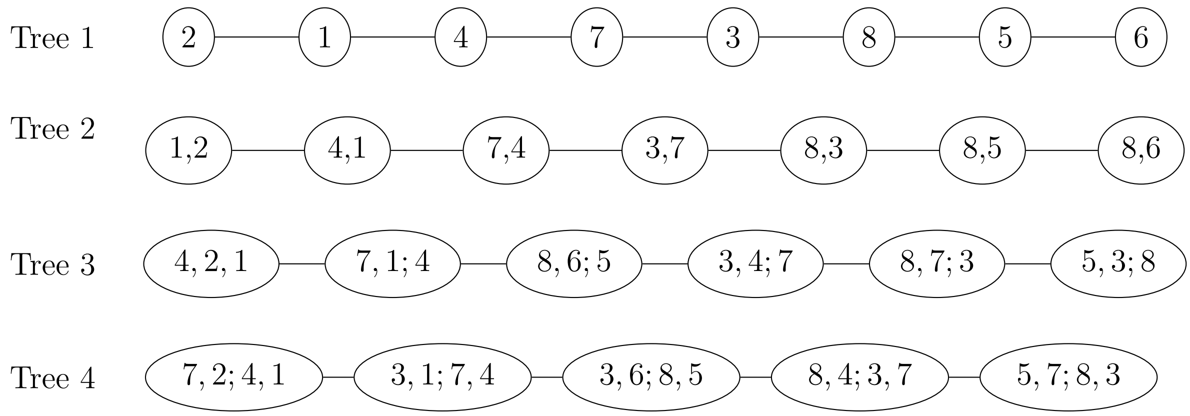

Figure 3: Trees 1-4 of the selected R-vine for $\{z_t^{(i)}\}, i = 1, 2, \ldots 8$

(i) Determine the spanning tree T_i that satisfies the proximity condition and maximizes the sum of absolute empirical Kendall's tau, i.e.,

$$\max_{E_i} \sum_{e=\{j,k;D\}\in E_i} |\hat{\tau}_{j,k;D}|,$$

where $\hat{\tau}_{j,k;D}$ is the empirical Kendall's tau between $F_{j|D}(y_j|\boldsymbol{y}_D)$ and $F_{k|D}(y_k|\boldsymbol{y}_D)$.

(ii) For each edge in the selected spanning tree T_i, estimate a collection of candidate bivariate copulas using MLE method and select the bivariate copula with the lowest BIC for the pairs of variables associated with this edge.

The standardized residual series $\{z_t^{(i)}\}$, $i = 1, , 2, \ldots, 8$, obtained from fitting an ARIMA-GARCH model to period components $\{\kappa_t^{(i)}\}$, are first transformed to pseudo observations using the empirical distribution functions. We apply the selection and estimation procedure to the pseudo observations. Since the pseudo observations are uniformly distributed on $[0, 1]$, the joint density function is the simply the product of bivariate copula densities. We limit the choices of bivariate copulas to commonly used ones including independent (I), Gaussian (N), Student's t (t), Clayton (C), Gumbel (G), Frank (F), Joe (J), and Survival Gumbel (SG) copulas. The first four trees of the selected R-vine are plotted in Figure 3. The selected tree structure is a special type of R-vine called D-vine whose trees are paths.

The estimated eight-dimensional R-vine copula is presented in Table 2, where *df* is the degree of freedom for t copula and par, tau, utd, and ltd represent the dependence parameter, Kendall's tau, upper tail dependence, and lower tail dependence of the estimated bivariate copula respectively. We observe from Table 2 that independent copula is selected more often for higher layers of the vine. None of the bivariate copulas in Tree 1 is independent, while all copulas in Tree 5 and above are independent. Since the spanning trees are sequentially selected to maximize dependence captured by each tree, Tree 1 is expected to model most dependence and thus contain most non-independent copulas. For the same reason, the Kendall's taus of the estimated bivariate copulas in Tree 1 are much higher than those in Tree 2 and above.

For comparative purpose, we also estimate an eight-dimensional t copula with 29 parameters including 28 correlation parameters and 1 degree of freedom. The loglikelihood and BIC of the estimated t copula are 182.3 and -227.76 respectively. Compared

Tree	Edge	Family	par	df	tau	utd	ltd
1	1,2	SG	1.60 (0.12)	-	0.38	-	0.46
	4,1	t	0.55 (0.07)	3.42 (1.54)	0.37	0.32	0.32
	5,6	N	0.50 (0.07)	-	0.33	-	-
	7,4	SG	1.48 (0.11)	-	0.33	-	0.40
	3,7	N	0.65 (0.05)	-	0.45	-	-
	8,3	F	3.91 (0.65)	-	0.38	-	-
	8,5	N	0.57 (0.06)	-	0.38	-	-
2	4,2;1	F	2.19 (0.61)	-	0.23	-	-
	7,1;4	SG	1.15 (0.08)	-	0.13	-	0.17
	8,6;5	I	-	-	0.00	-	-
	3,4;7	I	-	-	0.00	-	-
	8,7;3	I	-	-	0.00	-	-
	5,3;8	C	0.63 (0.16)	-	0.24	-	0.33
3	7,2;4,1	G	1.21 (0.08)	-	0.17	0.22	-
	3,1;7,4	I	-	-	0.00	-	-
	3,6;8,5	I	-	-	0.00	-	-
	8,4;3,7	I	-	-	0.00	-	-
	5,7;8,3	I	-	-	0.00	-	-
4	3,2;7,4,1	I	-	-	0.00	-	-
	8,1;3,7,4	I	-	-	0.00	-	-
	7,6;3,8,5	G	1.16 (0.08)	-	0.14	0.18	-
	5,4;8,3,7	F	1.34 (0.57)	-	0.14	-	-
5 and above	...	I	-	-	0.00	-	-
	logLik: 166.25		AIC: -304.5	BIC: -266.44			

Table 2: Estimated R-vine copula for $z_t^{(i)}, i = 1, 2, \ldots, 8$

to the estimated R-vine copula, the multivariate t copula improves the loglikelihood by 16.5 but at the cost of 15 more parameters.

4 Dynamic Vine Copula

4.1 Time-varying dependence structures

Time-varying dependence has been found to improve the performance of factor copula [Chen et al., 2017] and classical multivariate copulas [Wang et al., 2015] in modelling multi-population mortality. In this section, we examine whether R-vine copula will benefit from time-varying dependence as well.

To incorporate dependence dynamics in a R-vine copula, we allow the dependence parameters of the bivariate copulas associated with the vine to change over time. Patton [2006] proposes the following evolution for the dependence measure φ_t of a bivariate copula $C(u, v)$:

$$\varphi_t = \Lambda\left(a + b\varphi_{t-1} + \frac{d}{10}\sum_{j=1}^{10}|u_{t-j} - v_{t-j}|\right),$$

where $\Lambda = (1+e^{-x})^{-1}$ ensures that $\varphi_t \in (0,1)$ at all times. The right-hand side of the dependence dynamic contains an autoregressive term φ_{t-1} and a forcing variable defined as the mean absolute difference between u and v over the past ten observations. The expectation of the forcing variable is inversely related to the dependence between u and v. The expectation is zero under perfect positive dependence, 1/3 under independence, and 1/2 under perfect negative dependence. Wang et al. [2015] adopt a similar dependence dynamic for classical multivariate copulas and also use the past ten observations in the forcing variable. Neither Patton [2006] nor Wang et al. [2015] provide explanation on why the past ten observations are used to define the forcing variable. There is no reason to assume that this particular forcing variable is the most suitable. Therefore, we allow the number of past observations in the forcing variable to take any value in $\{1, 2 \ldots, 15\}$ and select the value that yields the best goodness of fit.

We propose the following dependence dynamic for the bivariate copula associated with edge e, $e = \{j, k; D\}$:

$$\begin{aligned}\Lambda^{-1}\left(\tau^{(t)}_{j,k;D}\right) =& a_{j,k;D} + b_{j,k;D}\Lambda^{-1}\left(\tau^{(t-1)}_{j,k;D}\right)\\ &+ d_{j,k;D}\frac{1}{s}\sum_{i=1}^{s}\left|F_{j|D}\left(y_j^{(t-i)}|\boldsymbol{y}_D^{(t-i)}\right) - F_{k|D}\left(y_k^{(t-i)}|\boldsymbol{y}_D^{(t-i)}\right)\right| \end{aligned} \tag{D1}$$

where $a_{j,k;D}$, $b_{j,k;D}$, and $d_{j,k;D}$ are the dynamic parameters to be estimated and $\Lambda(x) = (1+e^{-x})^{-1}$ such that $\tau^{(t)}_{j,k;D} \in (0,1)$. Since Table 2 shows that the estimated taus of the bivariate copulas associated with the selected R-vine are all positive, it is reasonable to use $(0,1)$ as the parameter space for $\tau^{(t)}_{j,k;D}$.

An alternative dependence dynamic for the bivariate copula associated with the edge $\{j, k; D\}$ was proposed by So and Yeung [2014] and expressed as follows:

$$\varphi^{(t)}_{j,k;D} = a_{j,k;D} + b_{j,k;D}\varphi^{(t-1)}_{j,k;D} + d_{j,k;D}\xi^{(t-1)}_{j,k;D},$$

where $\varphi^{(t)}_{j,k;D}$ can be Pearson correlation, Kendall's tau, or Spearman rank correlation for the pair of variables associated with the edge, and $\xi^{(t-1)}_{j,k;D}$ is the corresponding sample correlation between $y_j^{(t)}|\boldsymbol{y}_D^{(t)}$ and $y_k^{(t)}|\boldsymbol{y}_D^{(t)}$ calculated from the past s observations. $\xi^{(t-1)}_{j,k;D}$ can also be viewed as a forcing variable. However, this dependence dynamic does not ensure the right hand side always in the interval of $[-1, 1]$. To avoid this problem, we modify the dependence dynamic as follows:

$$\Lambda^{-1}\left(\tau^{(t)}_{j,k;D}\right) = a_{j,k;D} + b_{j,k;D}\Lambda^{-1}\left(\tau^{(t-1)}_{j,k;D}\right) + d_{j,k;D}\Lambda^{-1}\left(\xi^{(t-1)}_{j,k;D}\right), \tag{D2}$$

where $\Lambda(x) = \tanh(x)$ ensures that the conditional Kendall's tau remains in the interval of $(-1, 1)$. We cannot use the transformation function $\Lambda(x) = (1+e^{-x})^{-1}$ in (D2) because the sample Kendall's tau $\xi_{j,k;D}^{(t-1)}$ may be negative. When $|b_{j,k;D} + d_{j,k;D}| < 1$, $\Lambda^{-1}\left(\tau_{j,k;D}^{(t)}\right)$ is stationary and has a long-term mean of $a_{j,k;D}/(1 - b_{j,k;D} - d_{j,k;D})$. The value of s, the number of past observations used for calculating sample Kendall's tau, will be determined based on goodness of fit. Since the Kendall's tau $\tau_{j,k;D}^{(t)}$ is a one-to-one function of the bivariate copula parameter as shown in Table 8, equations (D1) and (D2) can also be viewed as the dynamics of bivariate copula parameter.

4.2 Estimation of the dynamic vine copulas

Assume that we have calculated the values of $F_{j|D}\left(y_j^{(t)}|\boldsymbol{y}_D^{(t)}\right)$ and $F_{k|D}\left(y_k^{(t)}|\boldsymbol{y}_D^{(t)}\right)$ using equation (2). Given the family of the bivariate copula family associated with the edge $\{j, k; D\}$, the parameters $a_{j,k;D}$, $b_{j,k;D}$, and $d_{j,k;D}$ can be estimated by maximizing the following loglikelihood:

$$\sum_t \ln c_{j,k;D}^{(t)}\left(F_{j|D}\left(y_j^{(t)}|\boldsymbol{y}_D^{(t)}\right), F_{k|D}\left(y_k^{(t)}|\boldsymbol{y}_D^{(t)}\right)\right),$$

where $c_{j,k;D}^{(t)}(.)$ is the bivariate copula density at time t with the copula parameter satisfying the dependence dynamic equation (D1) or (D2).

So and Yeung [2014] provide an estimation procedure for the dependence dynamics of a vine copula whose vine structure and associated bivariate copulas are known. We propose a generalized sequential procedure that does not require any prior information of the vine copula. Given a value of s for the forcing variable and the dynamic equation (D1) or (D2), we perform the following steps sequentially for Tree $i = 1, 2 \dots n-1$ to obtain the estimated dynamic R-vine copula:

i. For the ith tree, calculate the empirical Kendall's tau $\hat{\tau}_{j,k|D}$ for all conditional variable pairs $Y_j|\boldsymbol{Y}_D$ and $Y_k|\boldsymbol{Y}_D$ which are connected by an edge satisfying proximity condition.

ii. Select the spanning tree that maximizes the sum of absolute empirical Kendall's tau, i.e.,

$$\max_{E_i} \sum_{e=\{j,k;D\}\in E_i} |\hat{\tau}_{j,k;D}|.$$

iii. For the pairs of conditional variables associated each edge in the selected spanning tree T_i, select the best-fitting bivariate copula.

   (a) Test for independence

   - Calculate the empirical Kendall's tau between the pair of conditional variables and test the significance of Kendall's tau [1].

[1] Under the null hypothesis of independence, the sampling distribution of tau is approximated by a normal distribution with mean zero and variance $\frac{2(2n+5)}{9n(n-1)}$.

Dynamic (D1)						
s	3	4	5	6	7	10
logLik	212.93	215.66	225.33	225.31	212.90	219.16
AIC	−353.23	−353.26	−368.61	−368.56	−353.18	−356.26
BIC	−303.17	−303.92	−313.83	−313.78	−303.12	−301.48
Dynamic (D2)						
s	3	5	10	11	12	15
logLik	192.58	192.13	194.46	196.51	202.26	198.17
AIC	−321.98	−321.07	−337.17	−341.26	−343.34	−340.60
BIC	−276.64	−275.73	−299.27	−303.36	−300.71	−297.26

Table 3: Goodness of fit of the estimated dynamic R-vine copulas assuming different dependence dynamics and various values of s

- If the null hypothesis of independence cannot be rejected at the 5% significance level, independent bivariate copula is selected and we proceed to the next tree.
- If the null is rejected at the 5% significance level, we perform the remaining steps iii(b) and iii(c).

(b) For each candidate copula family, estimate both static and dynamic bivariate copulas for the pair of conditional variables.

(c) Select the copula with the lowest BIC among all estimated static and dynamic copulas.

We perform the above procedure for $s = 1, 2, \dots 15$ respectively and select the value of s that leads to the dynamic R-vine copula with the lowest BIC.

Table 3 compares the goodness of fit of the estimated dynamic R-vine copulas assuming different dynamic equations and various values of s. Using dynamic (D1), the lowest AIC and BIC are obtained at $s = 5$. Using dynamic (D2), the lowest AIC and BIC are obtained at $s = 11$. Overall, dynamic (D1) performs better than (D2) in terms of goodness of fit.

Table 4 presents the selected and estimated R-vine copulas using (D1) with $s = 5$ and (D2) with $s = 11$. Since our selection and estimation procedure determines whether dynamic or static bivariate copula should be used for each edge based on BIC, it is possible to have both dynamic and static bivariate copulas in the selected R-vine. When dynamic bivariate copula is selected for an edge, there are four estimated parameters ($a_{j,k;D}$, $b_{j,k;D}$, $d_{j,k;D}$, and df) for t copula and three ($a_{j,k;D}$, $b_{j,k;D}$, and $d_{j,k;D}$) for all other candidate copula families. When static bivariate copula is selected, only $a_{j,k;D}$ and/or df are estimated and $a_{j,k;D} = \Lambda^{-1}(\tau_{j,k;D})$.

Using dynamics (D1) and (D2), time-varying dependence is selected predominantly for the bivariate copulas associated with Tree 1. Since Tree 1 captures the most dependence among all trees, time-varying dynamic is most likely present in the dependence modelled by Tree 1. As we proceed to higher trees, less dependence is left to model and time-varying dynamic is less likely to be necessary.

The comparison of Tables 2 and 4 shows that the AIC and BIC of the two dynamic R-vine copulas are significantly lower than those of the static R-vine, thereby indicating that allowing time-varying dependences improves the performance of R-vine copula in modelling mortality dependence.

The dynamic and static R-vines select the same tree structure but different bivariate copula families for some edges. For example, the static R-vine selects t copula for the edge $\{4, 1\}$ in Tree 1 while both dynamic R-vines select survival Gumbel copula for the same edge. For each edge, the static R-vine estimates all candidate static bivariate copulas and selects the one with the lowest BIC while the dynamic R-vines estimate not only static but also dynamic bivariate copulas and select the one with the lowest BIC. Therefore, the selected bivariate copula families for the same edge in the static and dynamic R-vines are not necessarily the same.

Although both dynamic R-vines select static Gaussian copula for the edge $\{4, 2; 1\}$ in Tree 2, different parameter estimates are obtained. The bivariate copula associated with the edge $\{4, 2; 1\}$ is estimated from the conditional CDFs $F_{4|1}(y_4|y_1)$ and $F_{2|1}(y_2|y_1)$ which are calculated by the following equations:

$$F_{4|1}(y_4|y_1) = \frac{\partial C_{4,1}(F_4(y_4), F_1(y_1))}{\partial F_2(y_2)} \quad \text{and} \quad F_{2|1}(y_2|y_1) = \frac{\partial C_{1,2}(F_1(y_1), F_2(y_2))}{\partial F_1(y_1)}.$$

The two dynamic R-vines select different bivariate copulas for the edge $\{4, 1\}$ and obtain different estimates for $C_{4,1}(F_4(y_4), F_1(y_1))$, thereby leading to different values for the conditional CDF $F_{4|1}(y_4|y_1)$. For the same reason, the calculated values for $F_{2|1}(y_2|y_1)$ using the two dynamic R-vines are different as well. As a result, the parameter estimates for the bivariate copula associated with the edge $\{4, 2; 1\}$ in the two dynamic R-vines are different.

We also observe that the R-vine using (D2) selects dynamic bivariate copulas less often than the R-vine using (D1). Dynamic (D2) uses the sample correlation of the past 11 observations as the forcing variable while (D1) uses the mean absolute difference of past 5 observations. Both forcing variables can be viewed as a moving average of past data. When a longer period of past data is used in the moving average, the forcing variable has less variation and is less able to explain the changes of dependence. As a result, a bivariate copula with dynamic (D2) may not outperform a static bivariate copula for some edges.

In Figure 4, we plot the fitted Kendall's taus for the bivariate copulas associated with the edges in Tree 1. The solid and dashed lines represent the fitted taus using dynamics (D1) and (D2) respectively. When a static bivariate copula is selected for an edge, a horizontal line at the level of the estimated tau is plotted as the fitted Kendall's taus. In the panels for edges $\{5, 6\}$ and $\{7, 4\}$, the solid and dashed lines overlap because the two dynamic R-vines select the same static bivariate copula. The dashed lines are less jagged than the solid lines since the forcing variable in (D2) is calculated with a longer period of past observations and hence is smoother.

Tree	Edge	Dynamic (D1), $s=5$				Dynamic (D2), $s=11$			
		Family	$b_{j,k;D}$	$d_{j,k;D}$	$a_{j,k;D}$	Family	$b_{j,k;D}$	$d_{j,k;D}$	$a_{j,k;D}$
1	1,2	SG	1.08	0.98	-0.20	SG	1.09	-0.18	0.06
	4,1	SG	1.05	1.15	-0.19	SG	-	-	-0.57
	5,6	N	-	-	-0.70	N	-	-	-0.70
	7,4	N	-	-	-0.65	N	-	-	-0.65
	3,7	N	1.08	1.44	-0.28	N	1.06	-0.10	0.02
	8,3	N	1.09	2.18	-0.43	N	0.95	-0.19	0.09
	8,5	N	1.10	1.63	-0.27	N	-	-	-0.47
2	4,2;1	N	-	-	-1.36	N	-	-	-1.35
	7,1;4	G	-	-	-1.78	G	-	-	-1.88
	8,6;5	I	-	-	-	I	-	-	-
	3,4;7	I	-	-	-	I	-	-	-
	8,7;3	I	-	-	-	I	-	-	-
	5,3;8	N	1.12	2.46	-0.53	C	1.11	-0.23	0.02
3	7,2;4,1	N	1.06	0.45	-0.05	G	-	-	-1.25
	3,1;7,4	I	-	-	-	I	-	-	-
	3,6;8,5	I	-	-	-	I	-	-	-
	8,4;3,7	I	-	-	-	I	-	-	-
	5,7;8,3	J	-	-	-1.81	I	-	-	-
4	3,2;7,4,1	I	-	-	-	I	-	-	-
	8,1;3,7,4	I	-	-	-	I	-	-	-
	7,6;3,8,5	G	-	-	-1.88	I	-	-	-
	5,4;8,3,7	N	-	-	-1.90	I	-	-	-
5	8,2;3,7,4,1	I	-	-	-	I	-	-	-
	5,1;8,3,7,4	I	-	-	-	I	-	-	-
	4,6;7,3,8,5	N	-	-	-1.86	I	-	-	-

	Dynamic (D1), $s=5$	Dynamic (D2), $s=11$
logLik	225.33	196.51
AIC	-368.61	-341.26
BIC	-313.83	-303.36

Table 4: Parameter estimates of the selected dynamic R-vine copulas

4.3 Evaluating the time-varying pairwise dependence

Figure 4 plots the fitted Kendall's taus and demonstrates how the pairwise dependences evolve historically for the pairs associated with Tree 1. However, the fitted Kendall's taus in the higher tree levels represent dependences conditional on the conditioning sets. For example, $\tau^{(t)}_{j,k;D}$ is the dependence between j and k at time t conditional on D. $\tau^{(t)}_{j,k;D}$ does not provide a clear indication of the unconditional correlation between j and k.

To obtain the pairwise dependences without any conditioning set, we adopt the simulation approach proposed by So and Yeung [2014]. The following procedures are taken iteratively for $t = 1, 2, \ldots$:

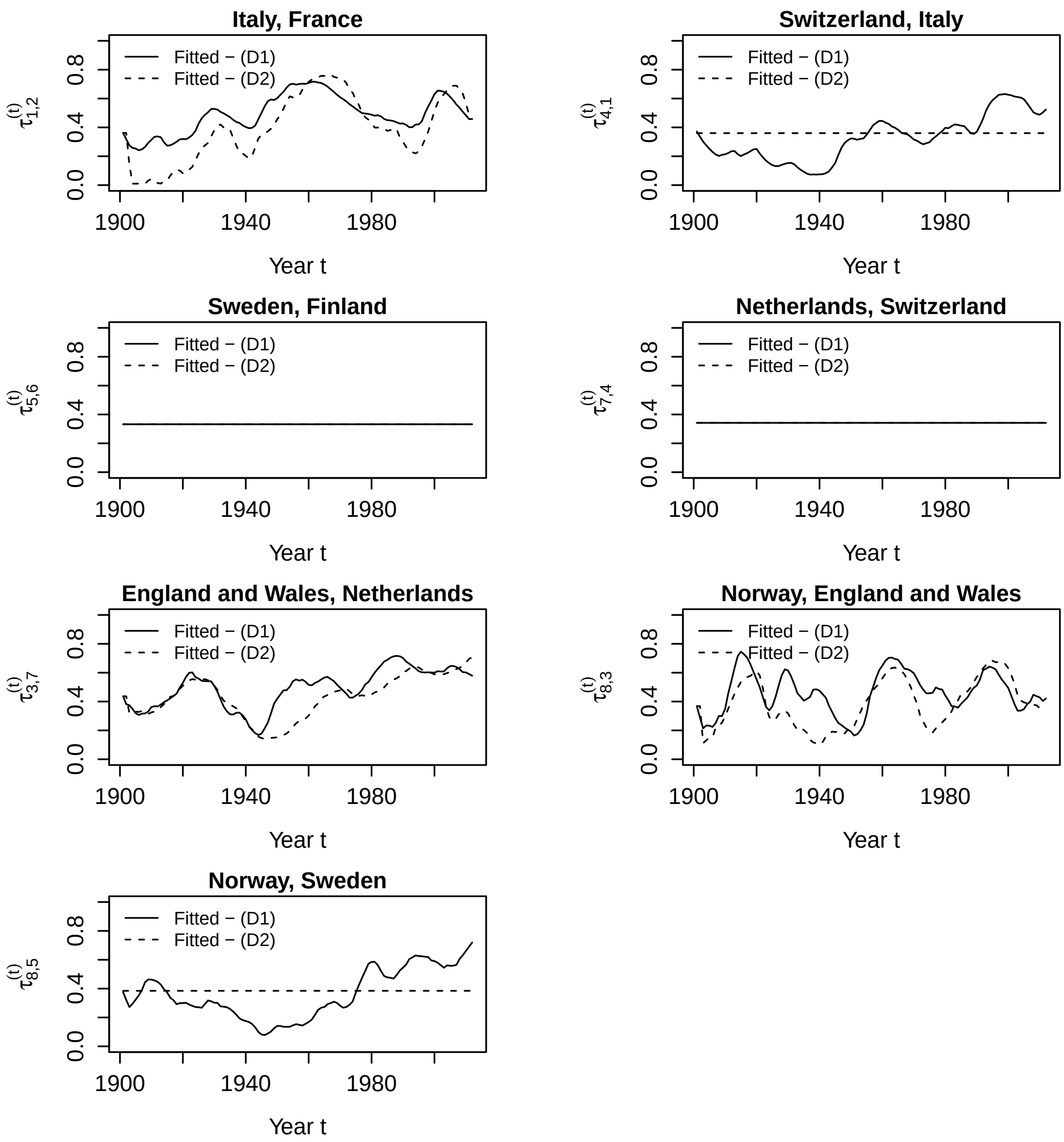

Figure 4: Fitted Kendall's taus for bivariate copulas associated with edges in Tree 1

i. Convert the fitted Kendall's tau for each edge to the corresponding bivariate copula parameter

ii. Construct a R-vine copula with the tree structure shown in Table 4 and the parameters obtained in Step i

iii. Simulate 5000 eight-dimensional uniform vectors from the constructed R-vine copula with the ith element of each vector as the simulated value for the ith variable

iv. Calculate the sample Kendall's tau for every pair of variables using the simulated vectors

Figure 5 presents the pairwise Kendall's taus computed using the simulation approach and the dynamic (D1). The curve of the computed taus for Italy and France are almost identical to that of the fitted $\tau_{1,2}^{(t)}$ in Figure 4, thereby suggesting that the simulation approach provides accurate estimation of pairwise correlations. We observe that the correlation between Italy and France is on average the highest among the twenty-eight pairs. Most pairs, such as France and the Netherlands, exhibit a moderate upward trend after 1945 which indicates that the correlation has been increasing slowly since 1945. An explanation for the upward trend could be the increasing globalization and cross-border movements. The computed correlations for Switzerland and the Netherlands show very small variation over time because the dynamic (D1) selects a static bivariate copula for the pair in Tree 1. Low variation is also observed for correlations between Sweden and Finland, between Switzerland and Sweden, and between Switzerland and Finland. The pair with the lowest average correlation over time is Italy and Norway. The computed Kendall's taus for this pair mostly lie between 0 and 0.2. The correlations between Switzerland and Norway, and between Italy and Finland are also below 0.2 for most periods.

Figure 6 presents the pairwise Kendall's taus computed using the simulation approach and the dynamic (D2). England and Wales and the Netherlands have the highest average correlation over time while Italy and France rank the second. The average correlation between Italy and Finland is 0.04, the lowest among the twenty-eight pairs. The average correlations between Sweden and Finland and between France and Finland are also very small at approximately 0.06. The comparison of Figures 5 and 6 shows that the dynamic (D2) leads to lower computed correlations and less steep upward trends after year 1945. The slower increase of correlation using the dynamic (D2) could be due to the longer period of past data used in the forcing variable of the dynamic (D2).

5 Mortality Forecast with Dynamic R-vine Copula

To forecast future mortalities of the eight populations, we simulate 5000 mortality paths based on the estimated APC model, ARIMA-GARCH model, and dynamic vine copula. The simulation of random vectors from static R-vine copula has been described by Dißmann et al. [2013]. To simulate random vectors from dynamic R-vine copula, an additional step for determining dependence parameters at each future time point is required. More specifically, the following steps are taken to simulate a mortality path using dynamic R-vine copula:

i. Let $t = 2013$.

ii. Determine $\tau^{(t)}_{j,k;D}$ for the pair of variables associated with the edge $\{j, k; D\}$ and calculate the corresponding bivariate copula parameter. If a dynamic bivariate copula is selected for this edge, $\tau^{(t)}_{j,k;D}$ is calculated using the dependence dynamic equation. If a static bivariate copula is selected for this edge, $\tau^{(t)}_{j,k;D}$ is equal to the tau of the estimated static bivariate copula.

iii. Repeat Step ii for all the edges in the selected R-vine.

iv. Construct an R-vine copula for time t with the vine structure and bivariate copula families shown in Table 4 and with the bivariate copula parameters obtained from Step iii.

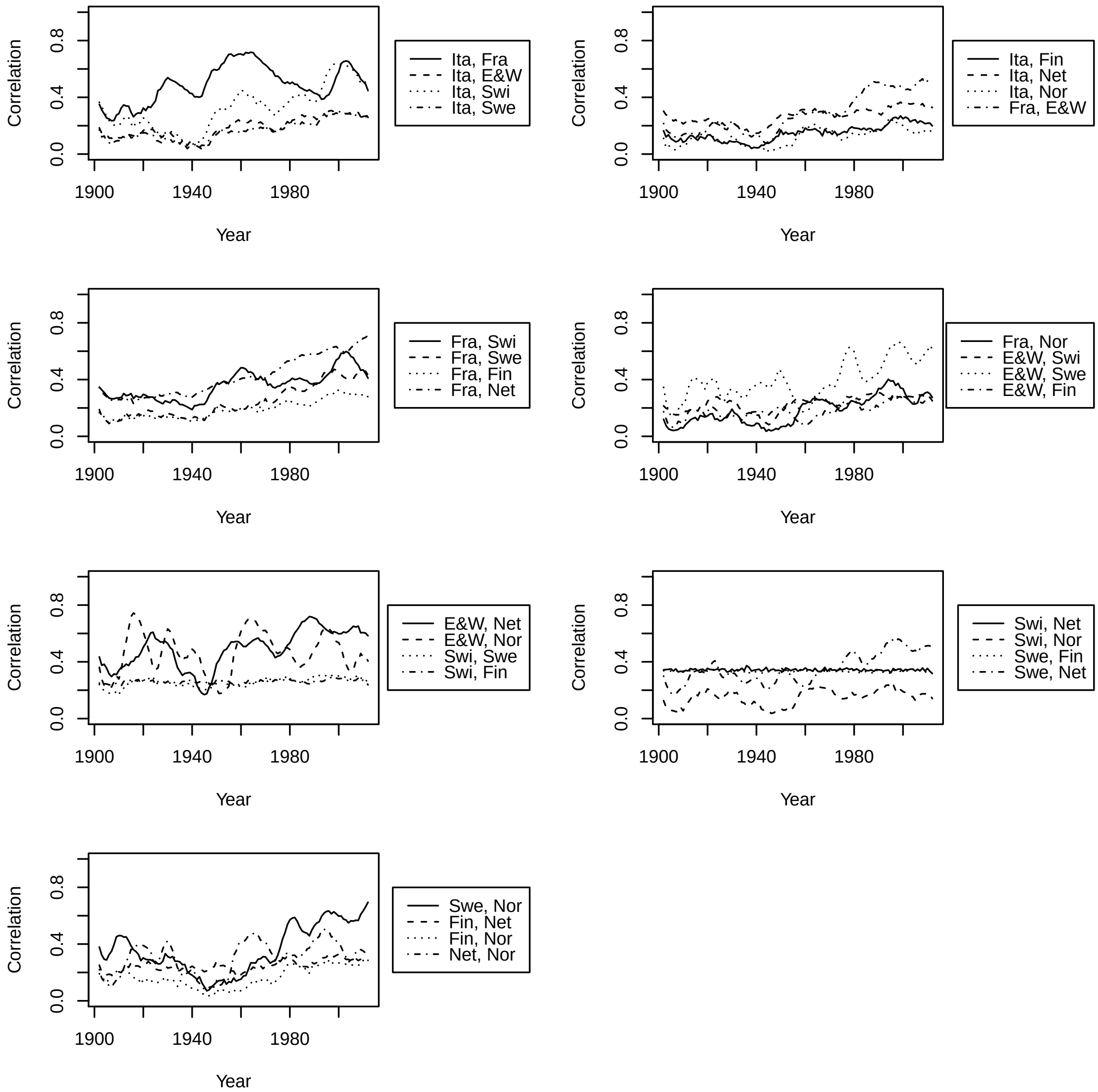

Figure 5: Computed historical pairwise correlations using the dynamic (D1)

v. Simulate an eight-dimensional uniform vector $\boldsymbol{u}$ from the R-vine copula constructed in Step iv following the procedure described by Dißmann et al. [2013].

vi. Transform the elements of $\boldsymbol{u}$ to standardized errors in the ARIMA-GARCH model. If the error distribution of $\kappa_t^{(i)}$ is normal, the simulated standardized error for $\kappa_t^{(i)}$ is $z_t^{(i)} = \Phi^{-1}(u_i)$ where u_i is the ith element of $\boldsymbol{u}$ and $\Phi^{-1}(.)$ is the inverse CDF of a standard normal distribution.

vii. Determine $\sigma_t^{(i)}$ and calculate $\kappa_t^{(i)}$ for $i = 1, 2, \ldots, 8$.

viii. Compute simulated mortality rate $m_{x,t}^{(i)}$, $i = 1, 2, \ldots, 8$, using the estimated APC model.

ix. Repeat Steps ii-viii for $t = 2014, 2015, \ldots$

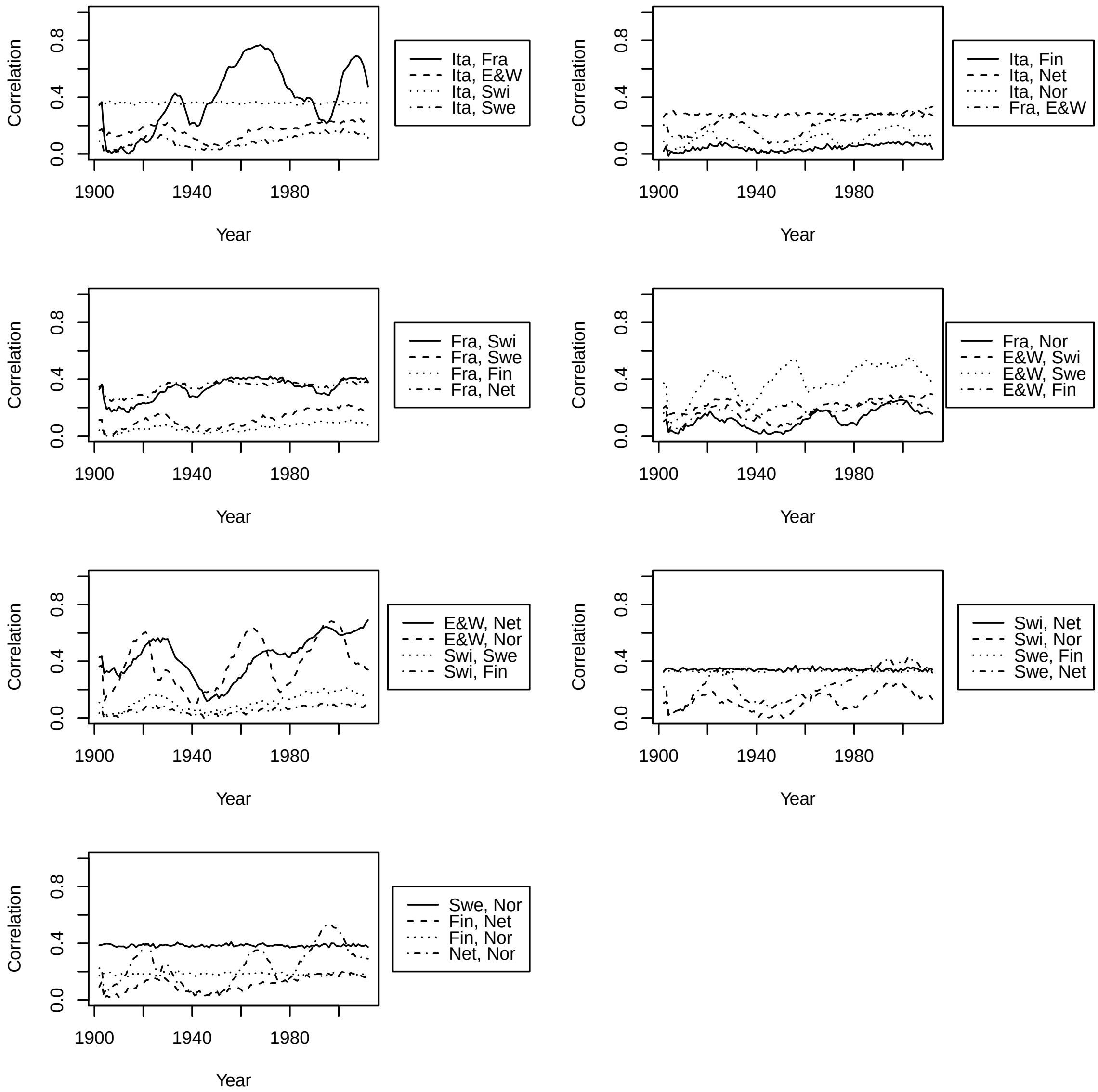

Figure 6: Computed historical pairwise correlations using the dynamic (D2)

We first simulate 5000 mortality paths using the R-vine copula with dynamic (D1). Figure 7 presents the fitted and simulated Kendall's taus for the pairs of variables associated with dynamic bivariate copulas in Tree 1. The fitted taus for years 1901-2012 are shown in solid lines and the simulated taus for years 2013-2027 are displayed using fan charts with 5%, 20%, 50%, 80%, 95% prediction intervals labelled out. The estimated taus from the static R-vine are also plotted in horizontal dashed lines for comparative purposes.

We observe significant differences between the forecasts of taus from the dynamic R-vine and the estimated taus from the static R-vine. Since dynamic (D1) is composed of an lag 1 autoregressive term and a forcing variable composed of the past five observations, the simulated taus are significantly impacted by the most recent fitted taus. For example, the mean forecast of tau for the edge $\{8, 5\}$ in 2013 is 0.73, very close to the fitted tau of 0.72 in 2012. The estimated static tau for this edge is 0.38, close to the average value of all fitted taus. Since the fitted taus of most recent years are higher than the corresponding estimated static taus for the edges plotted in Figure 7, the dynamic R-vine predicts higher dependences than the static R-vine for these edges in the short term. However, the difference decreases with time since the predicted taus using dynamic R-vine appear to decline with time.

We note that dynamic (D1) does not ensure stationarity for $\tau^{(t)}_{j,k;D}$. For example, the simulated taus for the edge $\{1, 2\}$ show a clear downward trend without sign of converging to a positive value. It is possible that the mean forecast of $\tau^{(t)}_{1,2}$ approaches zero as t goes to infinity. Since the downward slope is mild, the forecasts of $\tau^{(t)}_{1,2}$ are still in a reasonable range in 15 years as shown in Figure 7. However, we should be cautious about using this dynamic over a longer term.

We also simulate 5000 mortality paths using the R-vine copula with dynamic (D2). Figure 8 plots the fitted and simulated Kendall's taus for dynamic bivariate copulas associated with Tree 1 using dynamic (D2). The R-vine with dynamic (D2) also predicts higher dependences than the static R-vine for the edges plotted in Figure 8 in the short term. As t increases, the mean forecast of $\Lambda^{-1}(\tau^{(t)}_{j,k;D})$ converges to its long-term mean $a_{j,k;D}/(1 - b_{j,k;D} - d_{j,k;D})$. The long-term means for the edges $\{1, 2\}$, $\{3, 7\}$, and $\{8, 3\}$ are 0.65, 0.51, and 0.38 respectively, which convert to 0.83, 0.56, and 0.40 for $\tau^{(t)}_{j,k;D}$. The estimated taus from the static R-vine for these three edges are 0.38, 0.45, and 0.37 respectively. Therefore, the R-vine with dynamic (D2) will predict higher dependences than the static R-vine over the long term as well.

In addition, the comparison of Figures 7 and 8 shows that the simulated dependences using (D1) and (D2) are very different. Since there is no strong reason to exclude either of the dynamics, we consider both dynamics and compare their performances in the following analysis.

6 An Illustrative Longevity Hedge

When hedging longevity risk with standardized instruments, population basis risk often arises due to the different populations associated with the hedging instruments and the hedger's liability. Mortality dependence between these populations greatly impacts the extent of population basis risk and hence the effectiveness of the hedge. In this section, we illustrate how dynamic R-vine copula can be utilized to evaluate longevity hedge and examine how the choice of vine copula affects the assessed hedge effectiveness.

Suppose that an insurer sells annuities to 60-year-old individuals in the eight populations at the beginning of 2013, with 10,000 policies issued to each population. Each annuity policy makes regular payment of \$1 to a surviving annuitant at the beginning of each year starting from age 60. The last payment is made at the beginning of the year in which the annuitant dies or turns 89, whichever comes first.

The insurer enters into T-year S-forwards to hedge the uncertainty of its annuity liability in T years. An S-forward is an exchange of a realised survival rate of a given cohort in return for a fixed survival rate which is agreed upon at the outset of the contract. The insurer agrees to receive the realised survival rate and pay the fixed rate in S-forward contracts. Suppose that only S-forwards written on population (2)

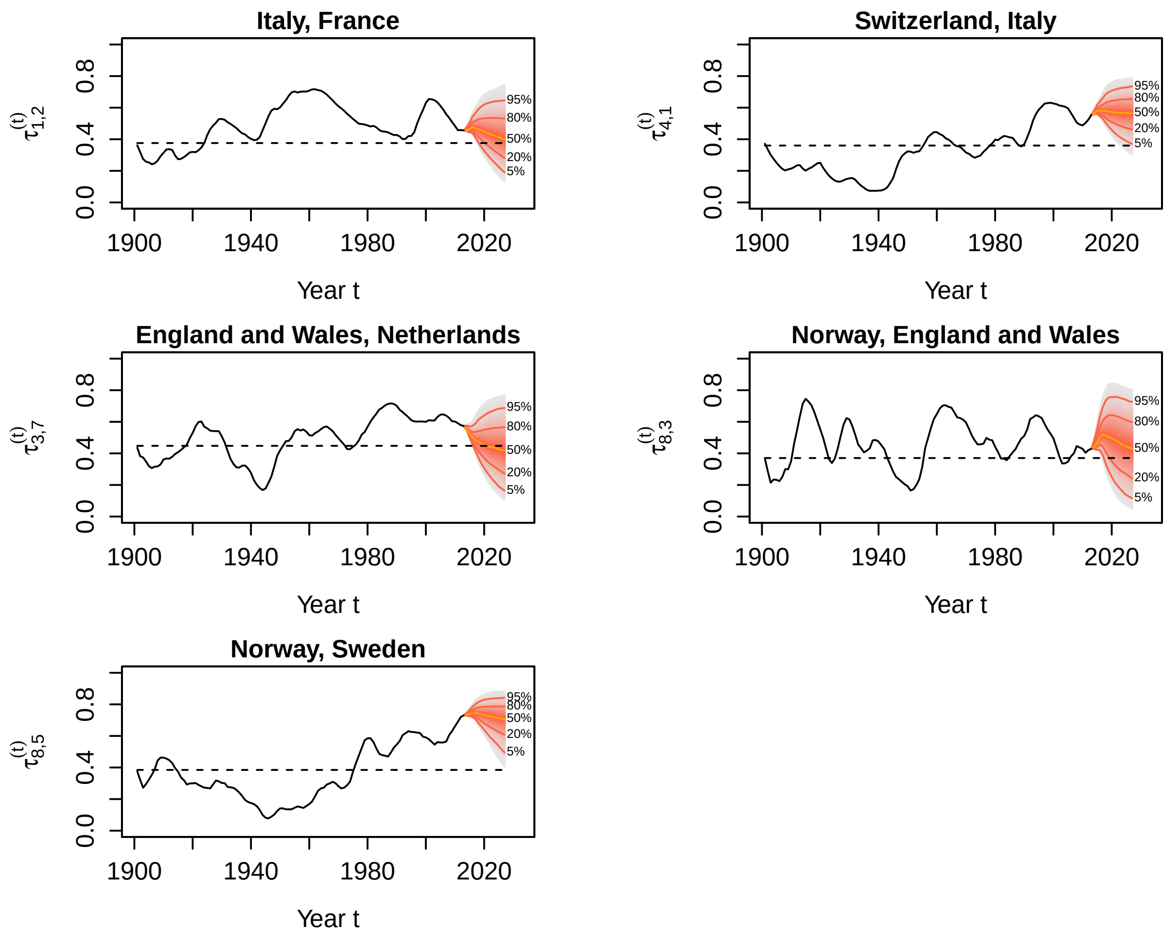

Figure 7: Fitted and simulated Kendall's taus for dynamic bivariate copulas associated with Tree 1 using the dynamic (D1)

England and Wales and population (7) Netherlands are available at the market.

Denote r as the annual effective interest rate. The payoff of the T-year S-forward on a cohort aged x_0 at t_0 from population (i) with a notional amount of $N^{(i)}$ can be written as $N^{(i)}H_T^{(i)}$, where

$$H_T^{(i)} = {}_Tp_{x_0,t_0}^{(i)} - {}_T\hat{p}_{x_0,t_0}^{(i)}, \ \ i = 2, 7,$$

and ${}_Tp_{x_0,t_0}^{(i)}$ and ${}_T\hat{p}_{x_0,t_0}^{(i)}$ are the T-year realized and fixed survival rates of this cohort. Assuming constant force of mortality between consecutive integer ages, ${}_tp_{x_0,t_0}^{(i)}$ can be approximated by ${}_tp_{x_0,t_0}^{(i)} = \prod_{k=0}^{t-1} e^{-m_{x_0+k,t_0+k}^{(i)}}$. We set $x_0 = 60$ and $t_0 = 2013$ for the S-forwards such that the cohorts underlying the S-forwards best match those underlying the annuity liability.

Denote $L_{x,t}^{(i)}$ as the number of surviving annuitants aged x at t from population (i). $L_{x_0,t_0}^{(i)} = 10,000$ for $i = 1, 2, \ldots, 8$. Assume that the number of deaths between t and $t+1$ follows Poisson distribution:

$$D_{x,t}^{(i)} \sim \text{Poisson} \ \ \left(L_{x,t}^{(i)}(1 - p_{x,t}^{(i)})\right).$$

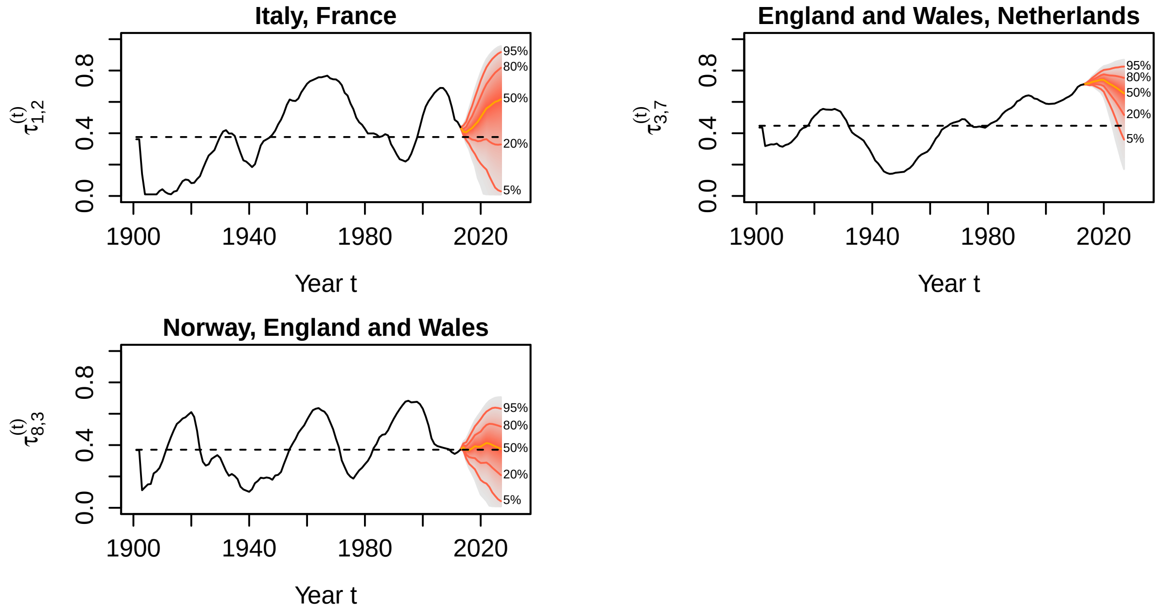

Figure 8: Fitted and simulated Kendall's taus for dynamic bivariate copulas associated with Tree 1 using the dynamic (D2)

The insurer's remaining annuity liability at time $t_0 + T$ can be written as follows:

$$LI_T = \mathbb{E}\left[\sum_{i=1}^{8}\sum_{j=0}^{29-T}(1+r)^{-j}L^{(i)}_{x_0+T+j,t_0+T+j}|\mathcal{F}_{t_0+T}\right],$$

where $\mathcal{F}_{t_0+T}$ contains all the information at time $t_0 + T$.

The hedge effectiveness is evaluated by the percentage of variance reduction which is defined as follows:

$$1 - \frac{\text{var}\left(H^{(2)}_T N^{(2)} + H^{(7)}_T N^{(7)} + LI_T|\mathcal{F}_{t_0}\right)}{\text{var}\left(LI_T|\mathcal{F}_{t_0}\right)}.$$

The insurer's hedging objective is to search for the optimal notional amounts $N^{(2)}$ and $N^{(7)}$ such the variance reduction is maximized.

We evaluate the hedge effectiveness under three cases:

i. allowing S-forwards to be written on both population (2) and population (7);

ii. allowing S-forwards to be written only on population (2), i.e. $N^{(7)}$ is restricted to 0;

iii. allowing S-forwards to be written only on population (7), i.e. $N^{(2)}$ is restricted to 0.

Figure 9 displays the maximum achievable variance reduction for the three cases. For each case, we plot the variance reduction under different hedge horizons and R-vine copulas. We observe that the static R-vine yields the lowest variance reduction in

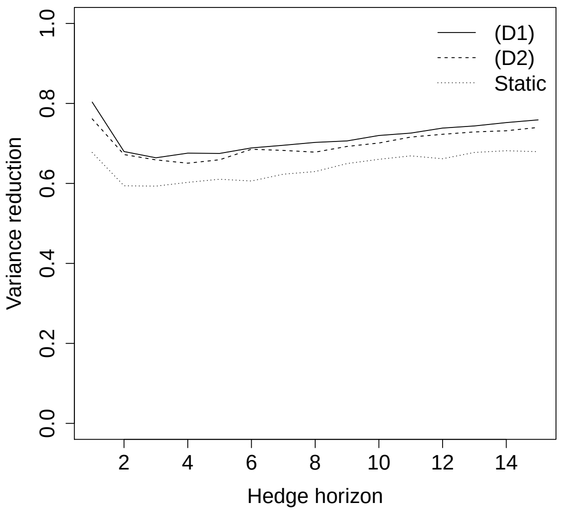

(a)

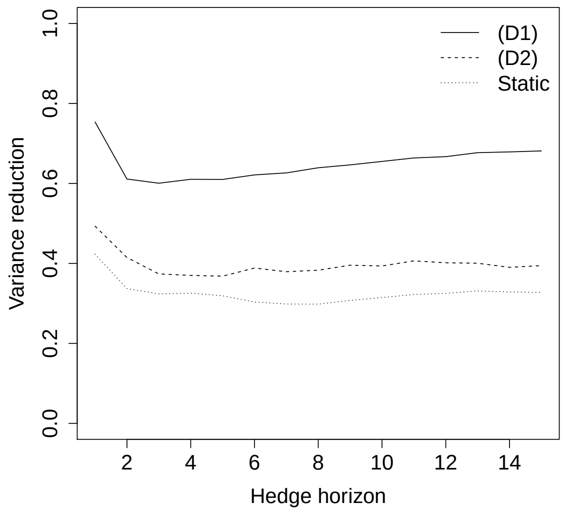

(b)

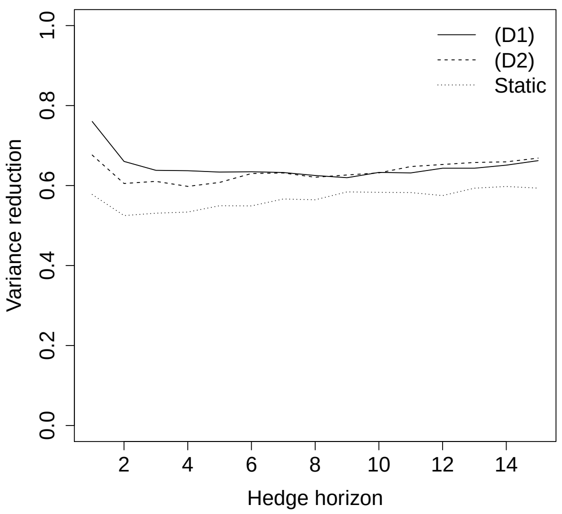

(c)

Figure 9: Panel (a): Allowing S-forwards to be written on both population (2) and population (7); Panel (b): Allowing S-forwards to be written only on population (2); Panel (c): Allowing S-forwards to be written only on population (7)

all three panels. Since Figures 7 and 8 indicate that the static R-vine predicts lower Kendall's taus and hence lower mortality dependences than the dynamic R-vines, the lower hedge effectiveness using the static R-vine is expected.

The comparison of Figures 7 and 8 also shows large difference between the predicted taus using the two dynamic R-vines. Therefore, we expect different hedge effectivenesses using the two dynamic vines as well. When S-forwards are allowed to be written only on population (2), there is significant difference between the hedge effectivenesses using the two dynamic R-vines as shown in Panel (b) of Figure 9. However, the effectiveness difference between the two dynamic R-vines is quite small in Panels (a) and

Regime 1						
Tree	Edge	Family	Parameter	tau	Tail dependence	
					Upper	Lower
1	2,3	N	0.65 (0.07)	0.45	-	-
	1,2	SG	2.17 (0.27)	0.54	-	0.62
	4,1	SG	1.98 (0.22)	0.50	-	0.58
2	1,3; 2	I	-	0.00	-	-
	4,2; 1	N	0.34 (0.11)	0.22	-	-
3	4,3; 1,2	I	-	0.00	-	-
Regime 2 - Independent						
$p_{11} = 0.91(0.06)$, $p_{22} = 0.75(0.13)$						
logLik=67.90, AIC=-123.8, BIC=-107.49						

Table 5: Estimated regime-switching R-vine copula using the mortality data of Italy, France, England and Wales, and Switzerland (Source: Zhou [2019])

(c). We observe from Figures 7 and 8 that the two dynamic R-vines predict different taus for each pair of variables, but the difference between the predicted taus is not uniform across the pairs of variables. It is possible that the two dynamic R-vines predict similar correlation for one pair of variables but very different correlation for another. As a result, the difference of hedge effectiveness between the two dynamic R-vines may be small when S-forwards are written on the survival rates of one cohort, but large when S-forwards are written on the survival rates of another cohort.

7 Comparison with Regime-Switching Vine Copulas

Zhou [2019] develops regime-switching vine copula to depict the evolution of mortality dependence. A regime-switching vine copula assumes that mortality dependence is determined by which regime the current period is in and the switching of regime follows an unobservable Markov process. The R-vines in different regimes have the same tree structure but different bivariate copulas associated with the edges. Zhou [2019] estimate a four-dimensional regime-switching R-vine to the male mortality data of Italy, France, England and Wales, and Switzerland. The estimated regime-switching R-vine copula are shown in Table 5.

To make a fair comparison between dynamic and regime-switching vine copulas, we use the same mortality data, base mortality model, and marginal model for the period components as Zhou [2019] but fit dynamic R-vine copulas instead. Table 6 presents the fitted dynamic R-vines using both (D1) and (D2). Both selected dynamic R-vines yield significantly lower BICs than the regime-switching R-vine.

Tree	Edge	Dynamic (D1), s=3				Dynamic (D2), s=11			
		Family	$b_{j,k;D}$	$d_{j,k;D}$	$a_{j,k;D}$	Family	$b_{j,k;D}$	$d_{j,k;D}$	$a_{j,k;D}$
1	2,3	G	1.06	0.67	-0.11	G	1.04	-0.05	0.01
	1,2	SG	1.09	0.75	-0.14	SG	1.09	-0.18	0.06
	4,1	N	1.05	1.40	-0.24	SG	-	-	-0.57
2	1,3; 2	I	-	-	-	I	-	-	-
	4,2; 1	N	-	-	-1.25	N	-	-	-1.35
3	4,3; 1,2	I	-	-	-	I	-	-	-

	Dynamic (D1), s=3	Dynamic (D2), s=11
logLik	83.13	82.41
AIC	-135.96	-141.95
BIC	-119.09	-127.08

Table 6: Estimated dynamic R-vine copulas using the mortality data of Italy, France, England and Wales, and Switzerland

8 Conclusion

In this paper, we apply dynamic R-vine copulas to capture the evolving mortality dependence. Dynamic R-vine is obtained by allowing time-varying dependence parameters for the bivariate copulas associated with a R-vine. Two time-varying dependence dynamics are proposed, each of which is a function of an autoregressive term and a forcing variable composed of certain number of past observations.

A generalized sequential procedure is presented to select R-vine structure, choose families for the bivariate copulas associated with the vine, determine whether static or dynamic bivariate copulas should be used, and estimate copula parameters. Applying this procedure to the male mortality data from eight populations, we obtain the estimated dynamic R-vine copulas. We further simulate future mortality paths using the estimated dynamic R-vines and evaluate the effectiveness of an illustrative longevity hedge with the simulated mortality paths. For comparative purposes, we perform the same analysis using a static R-vine copula.

We find that the dynamic R-vine copulas yield better goodness of fit than the static R-vine copula. The fitted dependences for recent years using dynamic R-vine copulas are much higher than the estimated dependence from the static R-vine. Since the fitted dependences exert positive influence on future dependences through the time-varying dependence dynamics, the dynamic R-vine copulas predict much higher dependences for future years and greater effectiveness for the illustrative longevity hedge than the static R-vine.

Although the R-vine copulas using the two proposed dependence dynamics yield similar levels of BIC, they lead to very different forecasts of future dependences and effectivenesses of longevity hedge. In particular, we observe that the estimated copula using the dynamic (D1) indicates faster increase of correlation and higher correlation levels from year 1945 than the copula using the dynamic (D2) for most population pairs. In this paper, we do not aim to select one dependence dynamic over the other. In the future research, we will consider backtesting to choose the most suitable dependence dynamic.

The same analysis is performed for the female mortality data from the eight countries. We do not present the detailed results in this paper since they lead to similar conclusions with those from the male mortality data. The dynamic R-vine copulas yield better goodness of fit and higher dependence forecasts than the static R-vine copula for the female data. The dynamic (D1) yields higher dependence forecasts and higher longevity hedge effectiveness than the dynamic (D2). However, the difference between the results using the two dynamics is smaller for the female data than for the male data. A milder increase of correlation over time is also observed in the female data than in the male data.

A Candidate Copula Families

Let $U_i = F_i(y_i)$, for $i = 1, 2, \ldots, n$. A copula CDF can be defined as

$$C(u_1, u_2, \ldots, u_n) = \Pr[U_1 \leq u_1, U_2 \leq u_2, \ldots, U_n \leq u_n].$$

Tables 7 and 8 present the CDF functions and dependence coefficients, respectively, of seven candidate copulas, including Independent (I), Gaussian (N), Student's t (t), Clayton (C), Gumbel (G), Frank (F), and Joe (J).

The following notations are used in Tables 7 and 8:

- R is the correlation matrix for the Gaussian or t copula;
- Φ_R is the joint CDF of an n-dimensional standard multivariate normal distribution with correlation matrix R and Φ_R^{-1} is the inverse CDF of the normal distribution;
- $T_{R,v}$ is the joint CDF of an n-dimensional standard multivariate Student's t distribution with v degrees of freedom and T_v^{-1} is the inverse CDF of the standard Student's t distribution.

Furthermore, we also consider survival Gumbel (SG) copula which is 180 degree rotated Gumbel. When rotating a bivariate copula by 180, the copula CDFs are given as follows:

$$C_{180}(u_1, u_2) \quad = \quad u_1 + u_2 - 1 + C(1 - u_1, 1 - u_2).$$

References

Kjersti Aas, Claudia Czado, Arnoldo Frigessi, and Henrik Bakken. Pair-copula constructions of multiple dependence. *Insurance: Mathematics and Economics*, 44: 182–198, 2009.

Family	$C(u_1, u_2, \ldots, u_n)$	Parameter
Independent (I)	$\prod_{i=1}^n u_i$	-
Gaussian (N)	$\Phi_R(\Phi^{-1}(u_1), \Phi^{-1}(u_2), \ldots, \Phi^{-1}(u_n))$	$R \in [-1,1]^{n\times n}$
Student's t (t)	$T_{R,v}(T_v^{-1}(u_1), T_v^{-1}(u_2), \ldots, T_v^{-1}(u_n))$	$R \in [-1,1]^{n\times n}$
Clayton (C)	$\left[\max\left\{\sum_{i=1}^n u_i^{-\theta} - n + 1, 0\right\}\right]^{-1/\theta}$	$\theta \in [-1,\infty) \setminus \{0\}$
Gumbel (G)	$e^{-\left(\sum_{i=1}^n (-\ln u_i)^\theta\right)^{1/\theta}}$	$\theta \in [1,\infty)$
Frank (F)	$-\frac{1}{\theta}\ln\left[1 + \frac{\prod_{i=1}^n (e^{-\theta u_i} - 1)}{e^{-\theta} - 1}\right]$	$\theta \in (-\infty,\infty) \setminus \{0\}$
Joe (J)	$1 - \left[1 - \prod_{i=1}^n (1 - (1-u_i)^\theta)\right]^{1/\theta}$	$\theta \in [1,\infty)$

Table 7: Copula functions and parameter domains of candidate copula families

Family	tau	Upper tail	Lower tail
Independent (I)	0	0	0
Gaussian (N)	$\frac{2}{\pi}\arcsin(\rho)$	0	0
Student's t (t)	$\frac{2}{\pi}\arcsin(\rho)$	$2t_{v+1}\left(-\sqrt{\frac{(v+1)(1-\rho)}{1+\rho}}\right)$	$2t_{v+1}\left(\sqrt{\frac{(v+1)(1-\rho)}{1+\rho}}\right)$
Clayton (C)	$\frac{\theta}{\theta+2}$	$2^{1/\theta}$	0
Gumbel (G)	$1 - \frac{1}{\theta}$	0	$2 - 2^{1/\theta}$
Frank (F)	$1 - \frac{4}{\theta} + 4\frac{\int_0^\theta \frac{x/\theta}{\exp(x)-1}dx}{\theta}$	0	0
Joe (J)	$1 + \frac{4}{\theta^2}\int_0^1 x\log(x)(1-x)^{\frac{2(1-\theta)}{\theta}}dx$	0	$2 - 2^{1/\theta}$

Table 8: Keadall's taus and tail dependences of candidate copula families

Tim Bedford and Roger M. Cooke. Probability density decomposition for conditionally dependent random variables modeled by vines. *Annals of Mathematics and Artificial Intelligence*, 32:245–268, 2001.

Tim Bedford and Roger M. Cooke. Vines–a new graphical model for dependent random variables. *The Annals of Statistics*, 30:1031–1068, 2002.

Eike C. Brechmann and Claudia Czado. Risk management with high-dimensional vine copulas: An analysis of the euro stoxx 50. *Statistics & Risk Modeling*, 30:307–342, 2013.

Andrew J. G. Cairns, David Blake, Kevin Dowd, Guy D. Coughlan, David Epstein, Alen Ong, and Igor Balevich. A quantitative comparison of stochastic mortality models using data from england and wales and the united states. *North American Actuarial Journal*, 13:1–35, 2009.

Andrew J. G. Cairns, David Blake, Kevin Dowd, Guy D. Coughlan, and Marwa Khalaf-Allah. Bayesian stochastic mortality modelling for two populations. *ASTIN Bulletin*, 41:29–59, 2011.

Hua Chen, Richard MacMinn, and Tao Sun. Multi-population mortality models: A factor copula approach. *Insurance: Mathematics and Economics*, 63:135–146, 2015.

Hua Chen, Richard D. MacMinn, and Tao Sun. Mortality dependence and longevity bond pricing: A dynamic factor copula mortality model with the gas structure. *Journal of Risk and Insurance*, 84:393–415, 2017.

Helena Chuliá, Montserrat Guillén, and Jorge M. Uribe. Modeling longevity risk with generalized dynamic factor models and vine-copulae. *ASTIN Bulletin*, 46:165–190, 2016.

Claudia Czado, Rainer Kastenmeier, Eike Christian Brechmann, and Aleksey Min. A mixed copula model for insurance claims and claim sizes. *Scandinavian Actuarial Journal*, 2012:278–305, 2012a.

Claudia Czado, Ulf Schepsmeier, and Aleksey Min. Maximum likelihood estimation of mixed c-vines with application to exchange rates. *Statistical Modelling*, 12:229–255, 2012b.

J. Dißmann, E. C. Brechmann, C. Czado, and D. Kurowicka. Selecting and estimating regular vine copulae and application to financial returns. *Computational Statistics & Data Analysis*, 59:52–69, 2013.

Kevin Dowd, Andrew J. G. Cairns, David Blake, Guy D. Coughlan, and Marwa Khalaf-Allah. A gravity model of mortality rates for two related populations. *North American Actuarial Journal*, 15:334–356, 2011.

Paul Embrechts, Filip Lindskog, and Alexander Mcneil. Chapter 8 - modelling dependence with copulas and applications to risk management. In Svetlozar T. Rachev, editor, *Handbook of Heavy Tailed Distributions in Finance*, volume 1 of *Handbooks in Finance*, pages 329 – 384. North-Holland, Amsterdam, 2003.

Tobias Michael Erhardt, Claudia Czado, and Ulf Schepsmeier. R-vine models for spatial time series with an application to daily mean temperature. *Biometrics*, 71:323–332, 2015.

Matthias Fischer, Christian Ḱock, Stephan SchlÃŒter, and Florian Weigert. An empirical analysis of multivariate copula models. *Quantitative Finance*, 9(7):839–854, 2009.

Edward W. Frees and Emiliano A. Valdez. Hierarchical insurance claims modeling. *Journal of the American Statistical Association*, 103:1457–1469, 2008.

Marius Hofert. Efficiently sampling nested archimedean copulas. *Computational Statistics & Data Analysis*, 55(1):57 – 70, 2011.

Harry Joe. Families of m-variate distributions with given margins and $m(m-1)/2$ bivariate dependence parameters. In Ludger Rüschendorf, Berthold Schweizer, and Michael D. Taylor, editors, *Distributions with fixed marginals and related topics*, volume Volume 28 of *Lecture Notes–Monograph Series*, pages 120–141. Institute of Mathematical Statistics, Hayward, CA, 1996.

Harry Joe. *Multivariate Models and Multivariate Dependence Concepts*. Monographs on Statistics and Applied Probability. Chapman & Hall/CRC, 1997.

David X. Li. On default correlation: A copula function approach. *The Journal of Fixed Income*, 9:43–54, 2000.

Johnny Siu-Hang Li and Mary R. Hardy. Measuring basis risk in longevity hedges. *North American Actuarial Journal*, 15:177–200, 2011.

Johnny Siu-Hang Li, Rui Zhou, and Mary Hardy. A step-by-step guide to building two-population stochastic mortality models. *Insurance: Mathematics and Economics*, 63: 121–134, 2015.

Nan Li and Ronald Lee. Coherent mortality forecasts for a group of populations: An extension of the lee-carter method. *Demography*, 42:575–594, 2005.

Eckhard Liebscher. Construction of asymmetric multivariate copulas. *Journal of Multivariate Analysis*, 99(10):2234 – 2250, 2008.

Tzuling Lin, Chou-Wen Wang, and Cary Chi-Liang Tsai. Age-specific copula-ar-garch mortality models. *Insurance: Mathematics and Economics*, 61:110–124, 2015.

Patricia Mariela Morillas. A method to obtain new copulas from a given one. *Metrika*, 61:169–184, 2005.

Ostap Okhrin, Yarema Okhrin, and Wolfgang Schmid. Properties of hierarchical archimedean copulas. *Statistics & Risk Modeling with Applications in Finance and Insurance*, pages 21–54, 2013.

Clive Osmond. Using age, period and cohort models to estimate future mortality rates. *International Journal of Epidemiology*, 14:124–129, 1985.

Andrew J. Patton. Modelling asymmetric exchange rate dependence. *International Economic Review*, 47:527–556, 2006.

Juan C. Reboredo and Andrea Ugolini. Downside/upside price spillovers between precious metals: A vine copula approach. *The North American Journal of Economics and Finance*, 34:84 – 102, 2015.

Juan Carlos Rodriguez. Measuring financial contagion: A copula approach. *Journal of Empirical Finance*, 14:401 – 423, 2007.

Abe Sklar. Fonctions de répartition àn dimensions et leurs marges. *Publications de l'Institut Statistique de l'Université de Paris*, 8:229–231, 1959.

Mike K. P. So and Cherry Y. T. Yeung. Vine-copula garch model with dynamic conditional dependence. *Computational Statistics & Data Analysis*, 76:672–686, 2014.

Chou-Wen Wang, Sharon S. Yang, and Hong-Chih Huang. Modeling multi-country mortality dependence and its application in pricing survivor index swaps - a dynamic copula approach. *Insurance: Mathematics and Economics*, 63:30–39, 2015.

Zihe Wang and Johnny Siu-Hang Li. A dcc-garch multi-population mortality model and its applications to pricing catastrophic mortality bonds. *Finance Research Letters*, 16:103–111, 2016.

Niall Whelan. Sampling from archimedean copulas. *Quantitative Finance*, 4(3):339–352, 2004.

Sharon S. Yang and Chou-Wen Wang. Pricing and securitization of multi-country longevity risk with mortality dependence. *Insurance: Mathematics and Economics*, 52:157–169, 2013.

Rui Zhou. Modelling mortality dependence with regime-switching copulas. *ASTIN Bulletin*, 49:373–407, 2019.

Rui Zhou, Johnny Siu-Hang Li, and Ken Seng Tan. Pricing standardized mortality securitizations: A two-population model with transitory jump effects. *Journal of Risk and Insurance*, 80:733–774, 2013.

Rui Zhou, Yujiao Wang, Kai Kaufhold, Johnny Siu-Hang Li, and Ken Seng Tan. Modeling period effects in multi-population mortality models: Applications to Solvency II. *North American Actuarial Journal*, 18:150–167, 2014.